

## Electronic Structure of Polyiodobenzenes

Igor Novak\* and Dong Bo Li

Department of Chemistry, National University of Singapore, Singapore 117543, Singapore

Branka Kovač

Physical Chemistry Division, "R. Bošković" Institute, HR-10000, Zagreb, Croatia

Received: October 16, 2001

The molecular and electronic structure of tri-, tetra-, and pentaiodobenzenes has been investigated by HeI/HeII photoelectron spectroscopy, high-level ab initio calculations and comparison with the spectra of chlorobenzene analogues.

### Introduction

The valence electronic structure of benzene and its derivatives had been studied extensively by UV photoelectron spectroscopy (UPS), because benzene is the archetypal aromatic compound. Halobenzenes were studied in particular detail<sup>1,2</sup> since the halogen substituents are monoatomic and small thus give rise to a relatively few, well resolved bands in the spectra. In addition, the spectra can be interpreted without considering different conformer populations. The number of possible halobenzenes is 1505, and naturally, only a small fraction of this number had been studied. Most halobenzenes studied to date are homosubstituted derivatives ( $C_6H_{6-n}X_n$ ; X = F or Cl) although some heterosubstituted ones were also reported.<sup>3–5</sup> Among the homosubstituted halobenzenes, a complete set of UPS data has been reported only for twelve fluoro<sup>6</sup> and twelve chlorobenzenes.<sup>7</sup> For bromo and iodobenzenes, only incomplete sets of UPS data are available.<sup>8,9</sup> In fluorobenzenes the interaction/perturbation of the aromatic ring's electronic structure by halogen lone pair ( $n_X$ ) is mostly inductive in nature while in chlorobenzenes<sup>7</sup> both mesomeric and inductive effects have been postulated. Nonetheless, in chloro and fluorobenzenes the  $\pi$ -ionization energy region (8.5–9.5 eV) of the spectra is always clearly separated from the halogen lone pair ionization region. This is rationalized by the energy difference between the aromatic  $\pi$ -orbitals and F2p- and Cl3p-orbitals. In iodobenzenes this energy difference is small and subsequently a much stronger  $n_X$ - $\pi$  interaction can be expected. Indeed, in mono and diiodobenzenes the overlap between  $\pi$  and I5p lone pair ionization manifolds was observed.<sup>9</sup> In this work we report the investigation of the electronic structure of additional members of iodobenzene family. We analyzed the effect of the increasing number of iodine substituents on the aromatic ring and also the relative influence of chlorine vs iodine on the aromatic ring by comparing chloro and iodobenzene analogues.

### Experimental and Theoretical Methods

**Synthesis.** Syntheses of 1,2,3-triodobenzene, 1,2,3,4-tetraiodobenzene, 1,2,3,5-tetraiodobenzene, and pentaiodobenzene were performed according to the procedures reported previously.<sup>10</sup> The syntheses of 1,2,4-triodobenzene, 1,3,5-triodobenzene, and 1,2,4,5-tetraiodobenzene have been performed according to the procedures in refs 11–13, respectively. The

identity and purity of the compounds prepared was checked by melting point measurements and by <sup>1</sup>H and <sup>13</sup>C NMR spectroscopy.

**Spectra.** The HeI/HeII photoelectron spectra of 1,2,3-triodobenzene (**1**), 1,2,4-triodobenzene (**2**), 1,3,5-triodobenzene (**3**), 1,2,3,4-tetraiodobenzene (**4**), 1,2,3,5-tetraiodobenzene (**5**), 1,2,4,5-tetraiodobenzene (**6**), and pentaiodobenzene (**7**) were recorded on the Vacuum Generators UV-G3 spectrometer and calibrated with small amounts of Xe gas which was added to the sample flow. The spectral resolutions in HeI and HeII spectra were 25 and 70 meV, respectively, measured as fwhm of <sup>2</sup>P<sub>3/2</sub> Ar<sup>+</sup> line. For compounds **1–7** elevated sample temperatures of 110, 100, 140, 180, 160, 180, and 230 °C, respectively, were required in order to achieve sufficient vapor pressures in the sample flow. The HeII spectrum of pentaiodobenzene and HeI/HeII spectra of hexaiodobenzene could not be measured due to the involatility of samples, which precluded generation of sufficient vapor pressures in the ionization chamber. The resolution of HeII spectra is always inferior to that in HeI, which implies that some bands that are well resolved in HeI have not been well resolved in HeII. The consequence for band intensities is that the measured intensities and intensity ratios sometimes refer to a combined intensity of two bands rather than to a single band.

**Calculations.** The ab initio calculations were performed with Gaussian 98 program.<sup>14</sup> The calculations were performed with full optimization at MP2(full) level using TZ2P basis set for all atoms except iodine for which SDD effective core potential set<sup>15</sup> was used. The iodine basis set includes relativistic effects which are important at high atomic numbers. Subsequently, a single-point calculation of ionization energies at MP2 geometry and with the same basis sets was performed by the ROVGF method.<sup>16</sup> Since the iodine lone pair manifolds can be expected to overlap and interact strongly with the ring  $\pi$ -orbitals thus giving high density of ionic states, it was necessary to proceed beyond Koopmans approximation and use Greens function method (ROVGF) for the calculation of ionization energies. The use of GF methods is well established in UPS<sup>17</sup> with the typical discrepancies between experimental and calculated ionization energies of 0.3 eV. The bands were deconvoluted using Gaussian profiles and baseline correction. The empirical relative intensity, RI(empir) for *i*th band was calculated as

$$RI_i = \{B_i^{\text{HeII}} \sum_i B_i^{\text{HeI}}\} / \{B_i^{\text{HeI}} \sum_i B_i^{\text{HeII}}\} \quad (1)$$

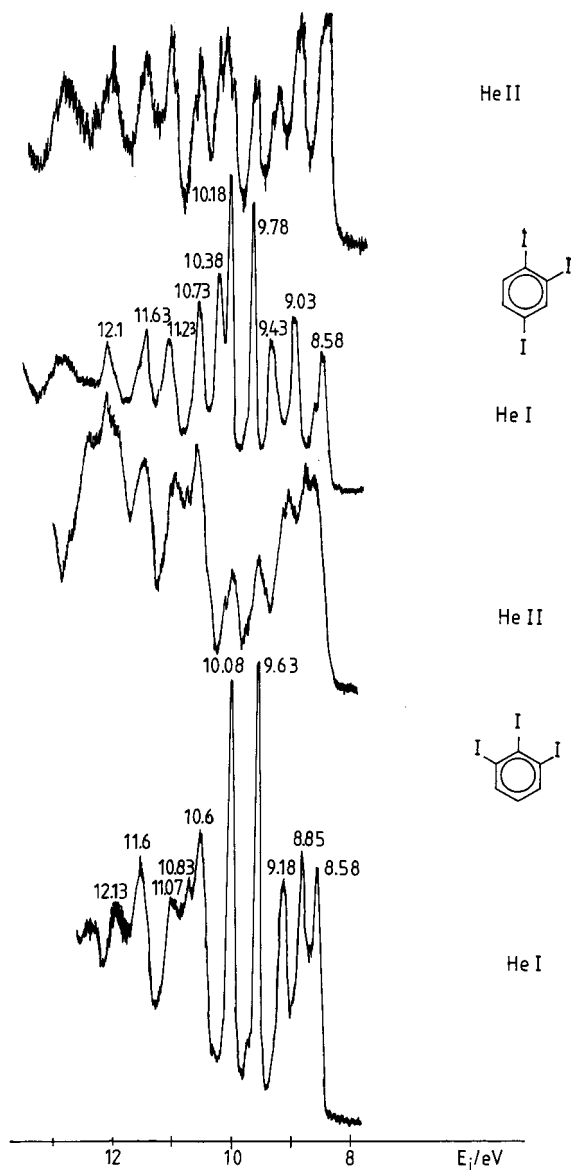


Figure 1. HeI/HeII photoelectron spectra of 1 and 2.

where  $B_i$  stands for the band intensity of  $i$ th band in HeI or HeII spectrum and the index of summation runs through the bands of interest. In our case the bands of interest were two ring  $\pi$ -ionizations and all iodine lone pairs. The RI value is the ratio of the intensity contribution of a particular band (in HeI or HeII spectrum) normalized by the total band intensity of the group of bands. The normalization is necessary because absolute band intensities could not be measured. RI(calcd) was also obtained from eq 1 using gross atomic populations and AO cross sections,<sup>18</sup> the populations were calculated with MOMix program<sup>19</sup> and the Ros-Schuit expression.<sup>20</sup>

## Results and Discussion

**Photoelectron Spectra.** The analysis of photoelectron spectra (Figures 1–4) is summarized in Figures 5 and 6 and Table 1. Figures indicate that the density of ionic states is large and the conclusions arrived at by several empirical and theoretical considerations must be compared if one is to obtain a reliable assignment.

The assignments take into account the following general principles.

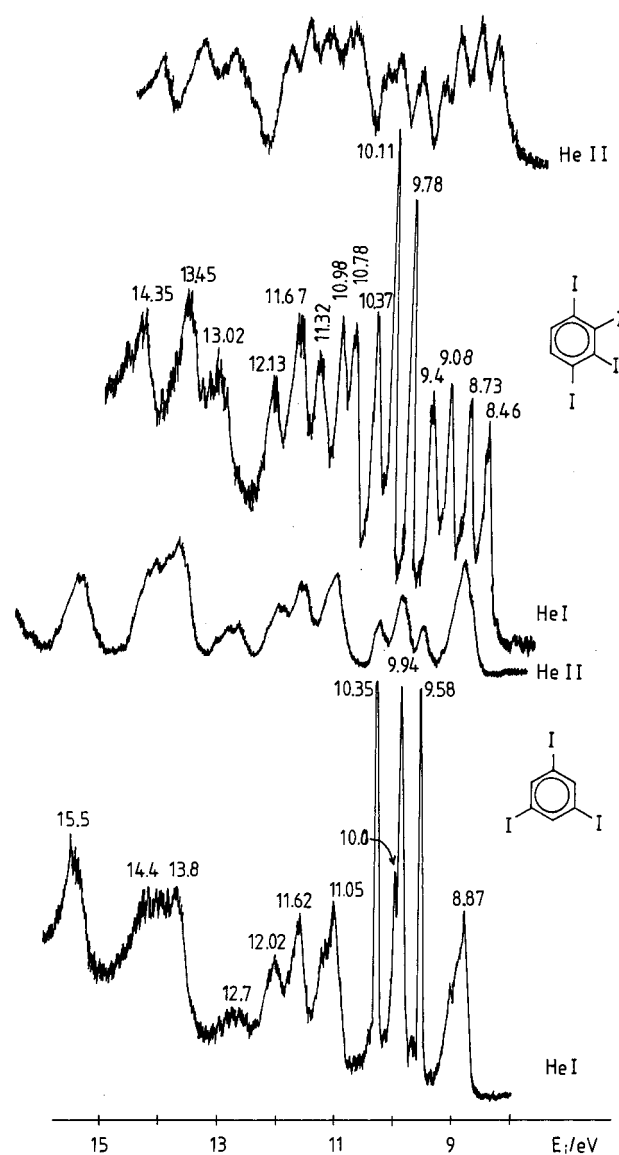


Figure 2. HeI/HeII photoelectron spectra of 3 and 4.

- The bands observed in the spectral region 8–11.5 eV correspond to ionizations from the ring  $\pi$ -orbitals ( $\pi$ ), the out-of-plane iodine lone pairs ( $\pi_I$ ), in-plane iodine lone pairs ( $\sigma_I$ ), or the combinations thereof.

- The relative intensity of bands RI(empir) corresponding to the ionizations from orbitals with the large I5p character decreases most prominently on going from HeI to HeII radiation. This is due to different energy dependence of the photoionization cross-sections for I5p- and C2p-orbitals.<sup>18</sup> The I5p cross section drops 3 times as much as that of C2p on going from HeI to HeII. Spatially diffuse  $\sigma_I$ -orbitals can acquire C2p character only by weak interaction with the energetically remote and spatially localized ring  $\sigma$ -orbitals. This leads to the working assumption that  $\sigma_I$ -orbitals can be expected to show greater reduction in relative HeII band intensity than  $\pi_I$ . Large, diffuse  $\pi_I$ -orbitals can, on the other hand, interact with energetically close and spatially delocalized ring  $\pi$ -orbitals and thus acquire some C2p character (leading to only a modest drop in relative HeII band intensity). Small RI(empir) values indicate  $\sigma_I$ -orbital character, intermediate values  $\pi_I$ , and large values  $\pi$ -orbital characters. RI(calcd) supports the assignment of HOMO and HOMO-1 bands as ring  $\pi$ -orbitals. The two lowest energy bands within  $\pi$ (ring)- $n_X$  manifold are also of  $\pi$ -type according to RI(calcd). However,

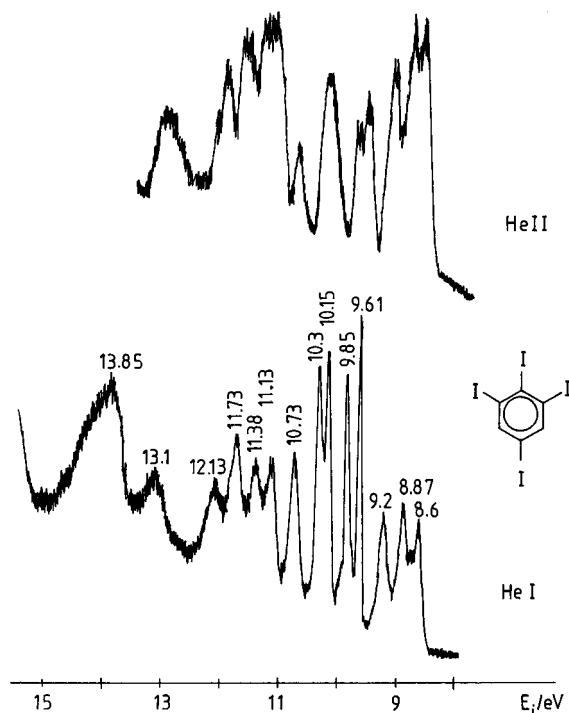


Figure 3. HeI/HeII photoelectron spectra of 5.

RI(calcd) is not useful/sensitive enough to distinguish other orbitals within the same manifold (Table 1).

- The sharp, narrow bands correspond to the ionization from strongly localized, nonbonding orbitals as suggested by the Franck–Condon principle.

- Comparison between a particular iodobenzene and its chloro analogue

- Absolute ordering of levels within iodine lone pair manifolds remains tentative due to the high density of corresponding ionic states (the states are often only 0.3 eV apart)

Additional assignment details for each molecule are described in the separate paragraphs below.

**Triiodobenzenes.** A total of eight orbital ionizations can be expected in the low energy region of triiodobenzenes: five  $\pi$ -type-ionizations from the out-of plane orbitals ( $\pi$ ,  $\pi_1$ ) and three in-plane localized  $\sigma$ -orbitals ( $\sigma_1$ ). Out of five  $\pi$ -type-ionizations, three originate from the nominally I5p lone pairs ( $\pi_1$ ) and two from the ring  $\pi$ -orbitals ( $\pi$ ). Please refer to Table 1 for all subsequent discussion.

In **1** the orbital symmetries are:  $\pi$ -type ( $a_2+b_1$ )-,  $\pi_1$ -type ( $a_2+2b_1$ )-, and  $\sigma_1$ -orbitals ( $a_1+2b_2$ ).

The symmetries indicate the possibility of  $\pi$ - $\pi_1$  mixing which can change the character of ring orbitals. Two sharp bands at 9.63 and 10.08 eV (Figure 1) show the most pronounced decrease in band intensity (RI) on going from HeI to HeII and can thus be readily assigned to  $\sigma_1$ -ionizations. The 9.18 eV band can then, also on the basis of RI measurements, be attributed to  $\pi_1$ -orbital. While this is not in complete agreement with GF calculations one should bear in mind that the calculations did not include all the relativistic effects so we propose as the final assignment the empirical one shown in Table 1. The empirical assignment is further supported by comparison with its chloro analogue. The replacement of chlorine with iodine leads to a small destabilization of ring  $\pi$ -orbitals and a much larger destabilization of iodine lone pairs. This comment applies to all the remaining iodobenzenes (Figures 5 and 6).

In **2** five bands can be expected to correspond to five  $\pi$ -type ( $a''$ )- and three to  $\sigma_1$ -type ( $a'$ )-ionizations. The bands at 9.43,

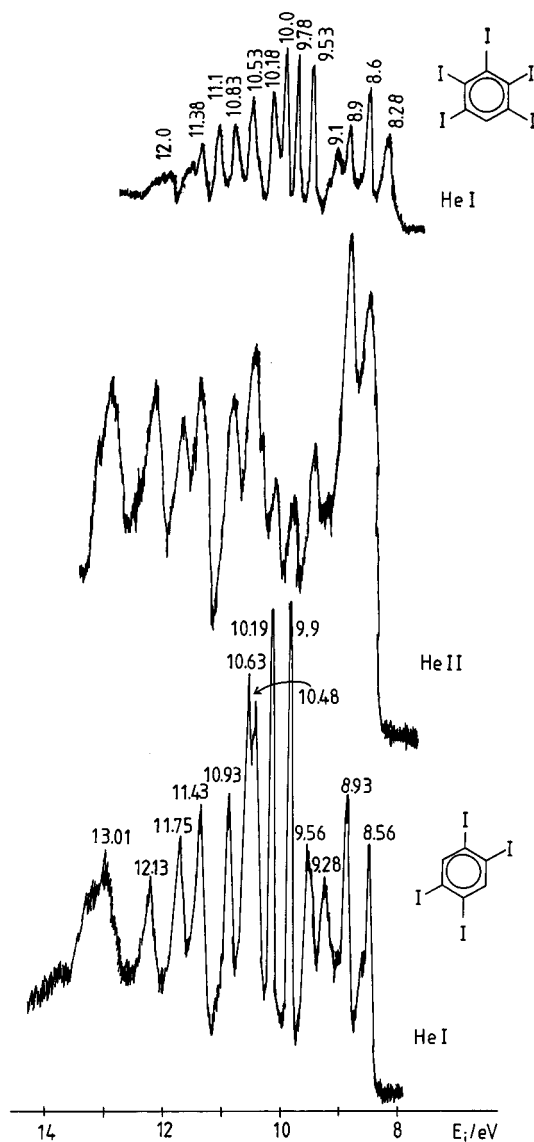


Figure 4. HeI/HeII photoelectron spectra of 6 and 7.

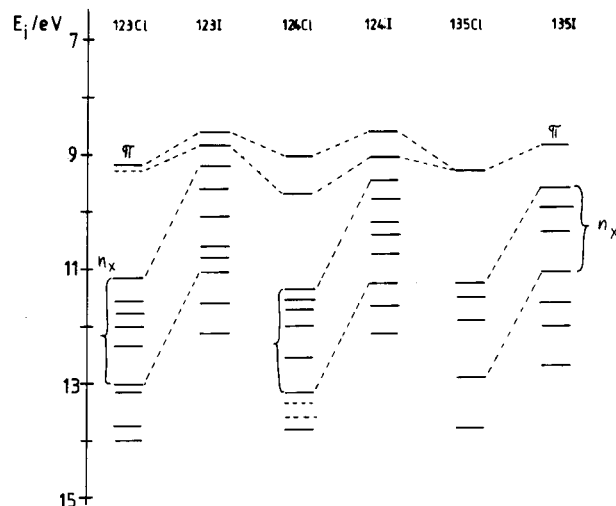
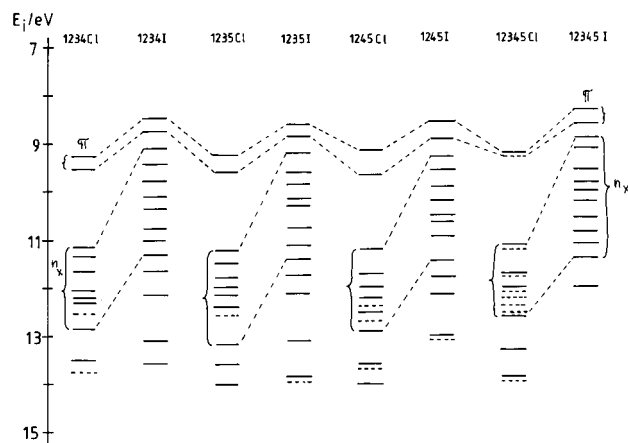


Figure 5. Energy level diagram of trichloro and triiodobenzenes.

10.78, and 10.18 eV show more pronounced intensity decrease (RI) than those at 10.38, 10.73, and 11.23 eV. The former can therefore be assigned to  $\sigma_1$ -type and the latter to  $\pi_1$ -type-ionizations. The large width of 9.43 eV band (considering that it is  $\sigma_1$ -type-ionization) may be attributed to it being an in-phase



**Figure 6.** Energy level diagram of tetrachloro, tetraiodo, pentachloro, and pentaiodobenzenes.

combination of in-plane I5p-orbitals. This observation provides some evidence for TS interactions of iodine lone pairs. The energy ranges of  $\sigma_1$ -manifolds in **1** and **2** are 0.98 and 0.75 eV, respectively. This is an indication of relative magnitudes of through-space I–I interactions. In **1** such interactions are stronger because of the presence of three vicinal iodines.

In **3** high  $D_{3h}$  symmetry leads to orbital degeneracy (reduction in the total number of bands) and the absence of through-space I–I interactions (Figure 2). Consideration of relative band intensities in the HeI spectrum leads to a straightforward assignment of  $\pi$ -ionization ( $e''$ ),  $\pi_1$ -ionization ( $e''$ ), and  $\sigma_1$ -ionization ( $e'$ ) (Table 1). However, the assignment of 9.58 and 10.35 eV bands to  $a_2''$  ( $\pi_1$ )- and  $a_2'$  ( $\sigma_1$ )-orbitals is not so definitive. We suggest the assignment given in Table 1, based on the calculations and comparison with the corresponding band profiles in the spectrum of **3** with its chloro analogue, 1,3,5-trichlorobenzene.<sup>7</sup>

The strong reduction of  $a_2''$  ( $\pi_1$ ) band intensity on going from HeI to HeII is worth noting because it appears to be an exception to the principles stated earlier. However, the  $a_2''$   $\pi_1$ -orbital cannot, for symmetry reasons, mix with the energetically close ring  $\pi$ -orbital  $e''$  (9.3 eV in benzene), but can only interact weakly with the energetically remote ring  $\pi$ -orbital  $a_2''$  (12.4 eV in benzene). Therefore, the  $a_2''$ -orbital at 9.58 eV retains largely I5p character (i.e., the  $\pi$ – $\pi_1$  interactions for the  $a_2''$ -orbital are symmetry allowed, but unfavorable on energy grounds). Another interesting observation concerns the appearance of shoulders at 8.87 and 11.05 eV bands. We suggest, on the basis of comparison with the spectrum of 1,3,5-trichlorobenzene,<sup>7</sup> that part of the band broadening could be due to Jahn–Teller splitting of the  $e''$  states of radical cations.

**Tetraiodobenzenes.** In the spectra of tetraiodobenzenes a total of 10 orbital ionizations can be expected in the low energy region: six  $\pi$ -type-ionizations from the out-of-plane orbitals ( $\pi$ ,  $\pi_1$ ) and four in-plane localized  $\sigma$ -orbitals ( $\sigma_1$ ). Out of the six  $\pi$ -type-ionizations, four originate from the nominally I5p lone pairs ( $\pi_1$ ) and two from the ring  $\pi$ -orbitals ( $\pi$ ).

In **4** (Figure 2) the relative HeI/HeII intensity changes (RI values) and band contours allow the assignment of  $\sigma_1$ -ionizations ( $2b_2+2a_1$ ) to bands at 9.40, 9.78, 10.11, and 10.37 eV. The remaining bands are assigned to  $\pi$ -ionizations ( $3a_2+3b_1$ ). The absolute ordering of levels was deduced from the calculations and comparison with the UPS of chloro analogue.

In **5** (Figure 3) the six  $\pi$ -ionizations ( $4b_1+2a_2$ ) and four  $\sigma_1$ -ionizations ( $3b_2+a_1$ ) can again be distinguished on the basis of HeI/HeII intensities, RI values, band profiles, and comparison

**TABLE 1: Vertical Ionization Energies ( $E_i \pm 0.03$  eV), Empirically, and Theoretically Derived Band Assignments, Calculated Ionization Energies (GF/eV), and Ratios of Measured Band Intensities at HeI/HeII Radiation (RI)**

compound (symmetry)	band	$E_i$	MO-type (empirical)	RI (empirical)	GF	MO-type (calcd)	RI (calcd)	
1 ( $C_{2v}$ )	X	8.58	$\pi$ ( $a_2$ )	1.80 <sup>a</sup>	8.42	$\pi$ ( $a_2$ )	1.42	
	A	8.85	$\pi$ ( $b_1$ )	1.80 <sup>a</sup>	8.50	$\pi$ ( $b_1$ )	1.41	
	B	9.18	$\pi_1$ ( $b_1$ )	1.24	8.63	$\sigma_1$ ( $b_2$ )	0.72	
	C	9.63	$\sigma_1$ ( $b_2$ )	0.65	9.50	$\pi_1$ ( $b_1$ )	0.61	
	D	10.08	$\sigma_1$ ( $a_1$ )	0.44	9.62	$\sigma_1$ ( $a_1$ )	0.79	
	E	10.60	$\sigma_1$ ( $b_2$ )	0.99 <sup>a</sup>	10.31	$\sigma_1$ ( $b_2$ )	0.74	
	F	10.83	$\pi_1$ ( $b_1$ )	0.99 <sup>a</sup>	10.53	$\pi_1$ ( $b_1$ )	1.28	
	G	11.07	$\pi_1$ ( $a_2$ )	1.56	10.77	$\pi_1$ ( $a_2$ )	1.22	
	2 ( $C_s$ )	X	8.58	$\pi$ ( $a''$ )	1.61	8.26	$\pi$ ( $a''$ )	1.19
		A	9.03	$\pi$ ( $a''$ )	1.32	8.78	$\pi$ ( $a''$ )	1.26
B		9.43	$\sigma_1$ ( $a'$ )	0.70	9.10	$\sigma_1$ ( $a'$ )	0.74	
C		9.78	$\sigma_1$ ( $a'$ )	0.54	9.58	$\pi_1$ ( $a''$ )	0.69	
D		10.18	$\sigma_1$ ( $a'$ )	0.65 <sup>a</sup>	9.63	$\sigma_1$ ( $a'$ )	0.72	
E		10.38	$\pi_1$ ( $a''$ )	0.65 <sup>a</sup>	10.12	$\sigma_1$ ( $a'$ )	0.77	
F		10.73	$\pi_1$ ( $a''$ )	0.98	10.35	$\pi_1$ ( $a''$ )	1.18	
G		11.23	$\pi_1$ ( $a''$ )	1.16	11.08	$\pi_1$ ( $a''$ )	1.27	
3 ( $D_{3h}$ )		X	8.87	$\pi$ ( $e''$ )	1.44	8.57	$\pi$ ( $e''$ )	1.23
		A	9.58	$\pi_1$ ( $a_2''$ )	0.43	9.42	$\pi$ ( $a_2''$ )	0.68
	B	9.94	$\sigma_1$ ( $e'$ )	0.53	9.56	$\sigma_1$ ( $a_2'$ )	0.66	
	C	10.35	$\sigma_1$ ( $a_2'$ )	0.45	9.73	$\sigma_1$ ( $e'$ )	0.78	
	D	11.05	$\pi_1$ ( $e''$ )	1.41	10.87	$\pi_1$ ( $e''$ )	1.22	
	4 ( $C_{2v}$ )	X	8.46	$\pi$ ( $a_2$ )	1.05	8.22	$\pi$ ( $a_2$ )	1.14
		A	8.73	$\pi$ ( $b_1$ )	1.01	8.41	$\sigma_1$ ( $b_2$ )	0.78
		B	9.08	$\pi_1$ ( $a_2$ )	0.96	8.53	$\pi$ ( $b_1$ )	1.18
		C	9.40	$\sigma_1$ ( $b_2$ )	0.55	9.23	$\sigma_1$ ( $a_1$ )	0.81
		D	9.78	$\sigma_1$ ( $a_1$ )	0.46	9.49	$\pi_1$ ( $a_2$ )	0.66
E		10.11	$\sigma_1$ ( $b_2$ )	0.41	9.55	$\pi_1$ ( $b_1$ )	0.74	
F		10.37	$\sigma_1$ ( $a_1$ )	0.43	10.06	$\sigma_1$ ( $b_2$ )	0.57	
G		10.78	$\pi_1$ ( $b_1$ )	0.85 <sup>a</sup>	10.49	$\sigma_1$ ( $a_1$ )	0.80	
H		10.98	$\pi_1$ ( $b_1$ )	0.85 <sup>a</sup>	10.68	$\pi_1$ ( $b_1$ )	0.99	
I		11.32	$\pi_1$ ( $a_2$ )	1.06	11.13	$\pi_1$ ( $a_2$ )	1.08	
5 ( $C_{2v}$ )	X	8.60	$\pi$ ( $b_1$ )	1.95	8.30	$\pi$ ( $b_1$ )	1.64	
	A	8.87	$\pi$ ( $a_2$ )	1.77	8.52	$\pi$ ( $a_2$ )	1.48	
	B	9.20	$\pi_1$ ( $b_1$ )	1.63	8.72	$\sigma_1$ ( $b_2$ )	0.78	
	C	9.61	$\sigma_1$ ( $b_2$ )	0.70	9.40	$\pi_1$ ( $b_2$ )	0.93	
	D	9.85	$\sigma_1$ ( $b_2$ )	0.50	9.66	$\sigma_1$ ( $b_2$ )	0.79	
	E	10.15	$\sigma_1$ ( $a_1$ )	0.57 <sup>a</sup>	9.69	$\sigma_1$ ( $a_1$ )	0.70	
	F	10.30	$\pi_1$ ( $b_1$ )	0.57 <sup>a</sup>	9.70	$\pi_1$ ( $b_1$ )	0.85	
	G	10.73	$\sigma_1$ ( $b_2$ )	0.45	10.40	$\sigma_1$ ( $b_2$ )	0.82	
	H	11.13	$\pi_1$ ( $a_2$ )	1.26 <sup>a</sup>	10.87	$\pi_1$ ( $a_2$ )	1.33	
	I	11.38	$\pi_1$ ( $b_1$ )	1.26 <sup>a</sup>	11.16	$\pi_1$ ( $b_1$ )	1.38	
6 ( $D_{2h}$ )	X	8.56	$\pi$ ( $b_{1g}$ )	1.99	8.21	$\pi$ ( $b_{1g}$ )	1.61	
	A	8.93	$\pi$ ( $b_{2g}$ )	2.11	8.58	$\pi$ ( $b_{2g}$ )	1.88	
	B	9.28	$\sigma_1$ ( $b_{1u}$ )	0.65	9.13	$\sigma_1$ ( $b_{1u}$ )	0.82	
	C	9.56	$\pi_1$ ( $b_{3u}$ )	0.96	9.16	$\sigma_1$ ( $b_{3g}$ )	0.81	
	D	9.90	$\sigma_1$ ( $b_{3g}$ )	0.46	9.46	$\pi_1$ ( $b_{3u}$ )	0.74	
	E	10.19	$\sigma_1$ ( $b_{2u}$ )	0.48	9.82	$\pi_1$ ( $a_u$ )	0.67	
	F	10.48	$\sigma_1$ ( $a_g$ )	0.95 <sup>a</sup>	10.01	$\sigma_1$ ( $b_{2u}$ )	0.79	
	G	10.63	$\pi_1$ ( $a_u$ )	0.95 <sup>a</sup>	10.25	$\sigma_1$ ( $a_g$ )	0.93	
	H	10.93	$\pi_1$ ( $b_{2g}$ )	1.05	10.63	$\pi_1$ ( $b_{2g}$ )	1.14	
	I	11.43	$\pi_1$ ( $b_{1g}$ )	1.08	11.27	$\pi_1$ ( $b_{1g}$ )	1.20	
7 ( $C_{2v}$ ) <sup>b</sup>	X	8.28	$\pi$ ( $a_2$ )		8.21	$\pi$ ( $a_2$ )		
	A	8.60	$\pi$ ( $b_1$ )		8.26	$\sigma_1$ ( $b_2$ )		
	B	8.90	$\pi_1$ ( $b_1$ )		8.37	$\pi$ ( $b_1$ )		
	C	9.10	$\sigma_1$ ( $b_2$ )		8.96	$\sigma_1$ ( $a_1$ )		
	D	9.53	$\sigma_1$ ( $a_1$ )		9.39	$\pi_1$ ( $b_1$ )		
	E	9.78	$\sigma_1$ ( $b_2$ )		9.51	$\pi_1$ ( $b_1$ )		
	F	10.00	$\sigma_1$ ( $a_1$ )		9.65	$\sigma_1$ ( $b_2$ )		
	G	10.18	$\sigma_1$ ( $b_2$ )		9.73	$\pi_1$ ( $a_2$ )		
	H	10.53	$\pi_1$ ( $b_1$ )		10.32	$\sigma_1$ ( $a_1$ )		
	I	10.83	$\pi_1$ ( $a_2$ )		10.58	$\sigma_1$ ( $b_2$ )		
J	11.10	$\pi_1$ ( $b_1$ )		10.76	$\pi_1$ ( $b_1$ )			
K	11.38	$\pi_1$ ( $a_2$ )		11.32	$\pi_1$ ( $a_2$ )			

<sup>a</sup> Average RI values for bands which could be resolved in HeI spectra, but not in HeII spectra. <sup>b</sup> HeII spectrum of **7** could not be measured hence no RI value is given in the Table 1.



**TABLE 2: The Energy Spreads of Halogen Lone Pair Manifolds in Tri-, Tetra-, and Pentachloro and iodobenzenes**

derivative	no. of pairs of vicinal halogen atoms	$\Delta E_X/\text{eV}$
1,2,3-Cl	2	1.82
1,2,3-I	2	1.89
1,2,4-Cl	1	1.82
1,2,4-I	1	1.80
1,3,5-Cl	0	1.69
1,3,5-I	0	1.47
1,2,3,4-Cl	3	1.70
1,2,3,4-I	3	2.24
1,2,3,5-Cl	2	1.98
1,2,3,5-I	2	2.18
1,2,4,5-Cl	2	1.67
1,2,4,5-I	2	2.15
1,2,3,4,5-Cl	4	1.48
1,2,3,4,5-I	4	2.48

with chlorobenzene analogue. The assignment of closely spaced bands to specific states is more difficult since the calculated ionization energies are of similar magnitude. The bands at 9.61, 9.85, and 10.73 show small RI values and thus correspond to three  $\sigma_1$ -ionizations. The fourth  $\sigma_1$ -ionization can be attributed to 10.15 eV band whose larger RI value arises from its overlap with the neighboring 10.30 eV band which has  $\pi_1$  character. The relative ordering of bands of each type has been deduced from MO calculations.

In **6** (Figure 4) the distinction between six  $\pi$ -ionizations ( $2b_{1g}+2b_{2g}+b_{3u}+a_u$ ) and four  $\sigma_1$ -ionizations ( $b_{1u}+b_{3g}+b_{2u}+a_g$ ) can again be made on the basis of HeI/HeII intensities (RI values). However, due to the large number of closely spaced bands (i.e. high density of ionic states), the final ordering of  $\pi_1$  and  $\sigma_1$  levels had to rely on calculations and is therefore somewhat tentative. The final assignment is summarized in Table 1.

In **7** (Figure 4) one can expect seven  $\pi$ -ionizations ( $4b_1+3a_2$ ) and five  $\sigma_1$ -ionizations ( $3b_2+2a_1$ ). The lack of HeII data (see Experimental section) necessitates the use of band profiles, MO calculations, and the comparison with pentachlorobenzene analogue as aids in the assignment (Table 1). These considerations make the proposed assignment for **7** less reliable than for other iodobenzenes in this work.

### Through-Space (TS) and Through-Bond (TB) Interactions

An interesting question arises when considering the electronic structure of chloro vs iodobenzenes. Which substituent, chloro or iodo, perturbs the electronic structure of the aromatic ring more profoundly? The first observation concerning UPS of chloro and iodobenzenes is that in the latter the lone pair bands are more widely spaced and thus better resolved. This may signify the increased lone pair-lone pair interactions in the latter. Lone pair-lone pair interactions can be conceived as being of TS- or TB-type. Data in Table 2 show the energy spread of lone pair manifolds in the two classes of halobenzenes and can help to quantify such interactions. In chlorobenzenes, TB interactions seem to predominate since the correlation between numbers of vicinal halogen lone pairs and energy spread is much poorer than that in iodobenzenes. In iodobenzenes the situation is reversed with TS interactions being more important. This can

also be seen from  $\pi$ -bands in iodobenzenes, which are better resolved than in chloro analogues and furthermore, have more asymmetrical profiles with prominent 0-0 transitions. This would suggest that  $n_X-\pi$  interactions are weaker in iodo than in chlorobenzenes. How is that possible in view of the energy proximity of  $n_X$ - and  $\pi$ (ring)-orbitals? 15p (lone pairs) have more diffuse electron density than Cl3p (chlorine lone pairs) and this may favor  $n_X-\pi$  interactions in the chlorobenzenes. The observed  $\pi$ -level destabilizations (Figures 5 and 6) on going from chloro to iodobenzene analogues can thus be assumed to be predominantly inductive in character.

### Conclusion

The iodobenzene molecules embody subtle and complicated intramolecular orbital interactions. Since they also contain heavy iodine atoms, the UPS data can serve as stringent bench test for full relativistic quantum chemical calculations. In addition, the experimental data which we have presented can provide encouragement for further development of various models of substituent effects.

### References and Notes

- (1) Bock, H.; Wittel, K. In *The Chemistry of Halides, Pseudohalides and Azides, Supplement D*; Patai, S., Rappoport, Z., Eds.; J. Wiley: Chichester, 1983; Chapter 28, p 1499.
- (2) Klasinc, L.; Novak, I.; McGlynn, S. P. In *The Chemistry of Halides, Pseudohalides and Azides, Supplement D2*; Patai, S., Rappoport, Z., Eds.; J. Wiley: Chichester, 1995; Chapter 4, p 123.
- (3) Mohraz, M.; Maier, J. P.; Heilbronner, E.; Bieri, G.; Shiley, R. H. *J. Electron Spectrosc. Relat. Phenom.* **1980**, *19*, 429.
- (4) Bieri, G.; Åsbrink, L.; von Niessen, W. *J. Electron Spectrosc. Relat. Phenom.* **1982**, *27*, 129.
- (5) Novak, I.; Potts, A. W. *J. Phys. Chem. A* **1998**, *102*, 3532.
- (6) Bieri, G.; Åsbrink, L.; von Niessen, W. *J. Electron Spectrosc. Relat. Phenom.* **1981**, *23*, 281.
- (7) (a) Ruščić, B.; Klasinc, L.; Wolf, A.; Knop, J. V. *J. Phys. Chem.* **1980**, *85*, 1486. (b) *J. Phys. Chem.* **1980**, *85*, 1490. (c) *J. Phys. Chem.* **1980**, *85*, 1495.
- (8) Potts, A. W.; Lyus, M. L.; Lee, E. P. F.; Fattahallah, G. H. *J. Chem. Soc., Faraday Trans. 2* **1980**, *76*, 556.
- (9) Cvitaš, T.; Güsten H.; Klasinc, L. *J. Chem. Soc., Perkin Trans. 2* **1977**, 962.
- (10) Mattern, D. L.; Chen, X. *J. Org. Chem.* **1991**, *56*, 5903.
- (11) Derbyshire, D. H.; Waters, W. A. *J. Chem. Soc.* **1950**, 3694.
- (12) Willgerodt, C.; Arnold, E. *Chem. Ber.* **1901**, *34*, 3343.
- (13) Mattern, D. L. *J. Org. Chem.* **1984**, *49*, 3051.
- (14) Frisch, M. J.; Trucks, G. W.; Schlegel, H. B.; Scuseria, G. E.; Robb, M. A.; Cheeseman, J. R.; Zakrzewski, V. G.; Montgomery, J. A., Jr.; Stratmann, R. E.; Burant, J. C.; Dapprich, S.; Millam, J. M.; Daniels, A. D.; Kudin, K. N.; Strain, M. C.; Farkas, O.; Tomasi, J.; Barone, V.; Cossi, M.; Cammi, R.; Mennucci, B.; Pomelli, C.; Adamo, C.; Clifford, S.; Ochterski, J.; Petersson, G. A.; Ayala, P. Y.; Cui, Q.; Morokuma, K.; Malick, D. K.; Rabuck, A. D.; Raghavachari, K.; Foresman, J. B.; Cioslowski, J.; Ortiz, J. V.; Stefanov, B. B.; Liu, G.; Liashenko, A.; Piskorz, P.; Komaromi, I.; Gomperts, R.; Martin, R. L.; Fox, D. J.; Keith, T.; Al-Laham, M. A.; Peng, C. Y.; Nanayakkara, A.; Gonzalez, C.; Challacombe, M.; Gill, P. M. W.; Johnson, B.; Chen, W.; Wong, M. W.; Andres, J. L.; Gonzalez, C.; Head-Gordon, M.; Replogle, E. S.; Pople, J. A. *Gaussian 98*, revision A.9; Gaussian, Inc.: Pittsburgh, PA, 1998.
- (15) Bergner, A.; Dolg, M.; Kuechle, W.; Stoll, H.; Preuss, H. *Mol. Phys.* **1993**, *80*, 1431.
- (16) Ortiz, J. V. *J. Chem. Phys.* **1988**, *89*, 6348.
- (17) von Niessen, W.; Dierksen, G. H. F.; Cederbaum, L. S. *J. Chem. Phys.* **1977**, *67*, 4124.
- (18) Yeh, J. J. *Atomic Calculation of Photoionization Cross-sections and Asymmetry Parameters*, Gordon and Breach: Langhorne, 1993.
- (19) Gorelsky, S. I.; Lever, A. B. P. *MOMix Program*; revision 4.4; York University: Toronto, Ontario, Canada, 2001.
- (20) Ros, P.; Schuit, G. C. A. *Theor. Chim. Acta* **1966**, *4*, 1.